CARBON 77 (2014) 790–795

Available at www.sciencedirect.com

ScienceDirect

journal homepage: www.elsevier.com/locate/carbon

Ion irradiation for improved graphene network formation in carbon nanotube growth

E.C. Neyts *, A. Bogaerts

University of Antwerp, Research Group PLASMANT, Department of Chemistry, Universiteitsplein 1, 2610 Wilrijk-Antwerp, Belgium

ARTICLE INFO

Article history:
Received 8 January 2014
Accepted 30 May 2014
Available online 11 June 2014

ABSTRACT

Ion irradiation of carbon nanotubes very often leads to defect formation. However, we have recently shown that Ar ion irradiation in a limited energy window of 10–25 eV may enhance the initial cap nucleation process, when the carbon network is in contact with the metal nanocatalyst. Here, we employ reactive molecular dynamics simulations to demonstrate that ion irradiation in a higher energy window of 10–35 eV may also heal network defects after the nucleation stage through a non-metal-mediated mechanism, when the carbon network is no longer in contact with the metal nanocatalyst. The results demonstrate the possibility of beneficially utilizing ions in e.g. plasma-enhanced chemical vapour deposition of carbon nanotubes.

1. Introduction

Carbon nanotubes (CNTs) hold promise for a multitude of applications, including sensors, transparent electrodes, interconnects, supercapacitors, transistors, energy storage applications, filters and membranes, high-strength materials, biomedical applications, and many more [1,2]. Key to many of these applications is the requirement to precisely tailor the structure of the CNTs. The intrinsic properties of the CNTs indeed depend on this structure, which in turn results from the details of the growth process. Unfortunately, it is at present not clear how the growth process and therefore the CNT structure can be controlled exactly.

The CNT structure and properties can also be tailored, altered and modified by the use of energetic species beams, including gamma rays [3,4], electrons [5,6] and ions [7–9]. Indeed, irradiation-induced modification of the graphitic network allows to introduce the specific functionalities needed for specific applications [10–13,7,14–21], for instance for enhancing CNT field emission [13,14], production of CNT quantum dots [20] and the fabrication of nanotube-based composites [21].

Moreover, the interaction of ions and electrons with CNTs is also of importance for the growth by plasma enhanced chemical vapor deposition (PECVD), in which ion and electron bombardment occur naturally [22,23]. This affects not only the properties of the resulting tubes, but most importantly the growth process itself. Gohier et al. for instance investigated the PECVD growth of single walled and multiwalled CNTs, and concluded that ion bombardment is a limiting factor in growing especially single walled CNTs using PECVD [24]. On the other hand, we recently demonstrated by using combined simulations and experiments, that ion bombardment in a limited energy window of 10–25 eV actually enhances the graphitic network growth in the nucleation stage [25]. At higher energies, we observed that ion bombardment destructs the network and thus inhibits the growth.

In view of the importance of ion-irradiation induced modification of CNTs (both for the properties and the growth process), many researchers investigated the nature of CNT ion

* *Corresponding author.*
E-mail address: erik.neyts@uantwerpen.be (E.C. Neyts).
http://dx.doi.org/10.1016/j.carbon.2014.05.083
0008-6223/

irradiation. Defects were identified as the origin of irradiation induced structural modifications [21,26–29], and defect formation has thus received considerable attention, both by experiments [3–6,8,9] as well as by simulations [11,7,29–38].

Very recently, O'Brien et al. performed molecular dynamics (MD) simulations to study the effect of carbon ion irradiation of CNT bundles on their mechanical properties, in the range 50–300 eV/atom [39]. Also Salonen et al. and Pomoell et al. investigated ion-irradiation induced defects in CNT bundles by classical MD [33,40], in the range 100 eV–1 keV. Xu et al. used MD simulations to probe the stability of single walled CNTs under Ar^+ and C^+ irradiation in the energy range 25 eV–1 keV [30,31]. In these simulations, it was shown that also the chemical nature of the impinging species plays a role in the damage creation. Finally, Pregler and coworkers [41,42] investigated ion beam irradiation, by 50 eV Ar^+ and CF_3^+ ions and 80 eV Ar^+ ions, of MWCNTs and nanotube based composites, again using MD simulations, demonstrating that ion bombardment effectively promotes intershell crosslinking.

Almost all of these studies, however, relate to rather high energy ion bombardment (several tens of eV and up), focussing on defect formation. Only a few researchers also studied defect healing [43–46], but in all cases in the context of a metal-mediated process and without dealing with ion bombardment.

At lower energies (below 30 eV), however, defects in the nucleating network may also be healed by ion bombardment, which then enhances the formation of the cap structure during the initial nucleation stage [25]. It thus appears that during the CNT nucleation stage, a balance exists between defect healing and defect creation by ion bombardment, and moreover that one could tune this balance by means of the ion energy. One may therefore ask: "Does ion bombardment also heal defects after the initial nucleation stage, when the carbon network is no longer in contact with the metal nanocatalyst?" Here we use MD simulations as outlined below to answer this question.

2. Methodology

We employ reactive MD simulations to investigate the dynamics of the ion-irradiation induced processes. We start with a fully detached CNT cap structure on a surface-bound Ni_{40} cluster, generated in a previous study on the vertical alignment effect of electric fields during single walled CNT growth [47]. This structure is thermalized at 1000 K employing the Berendsen heat bath with a relaxation constant of 250 fs. This initial structure is shown in Fig. 1a. Note that in contrast to our previous simulations, in which the number of defects in the tubes is minimized [45,46], we here deliberately start from defective tubes. We subsequently bombard this defective structure using Ar^+ ions with energies in the range 10–50 eV, for 200 consecutive impacts. After each impact, the structure is rethermalized to 1000 K, to remove excess heat from the system. In the MD simulation, the ions are modeled as fast neutrals, as justified by Auger neutralization of the incoming ion.

Atomic trajectories are integrated using the velocity verlet integrator. We model the Ni–Ni, Ni–C and C–C interactions by the Reax Force Field [48], using parameters developed by Mueller et al. [49]. The Ar–Ni and Ar–C interactions are modeled by means of a Molière potential using Firsov constants, as we have previously done in other studies investigating Ar-irradiation of carbon nanostructures [50,51]. We carried out ten independent simulation runs at each energy, to collect statistics on the data and to average the global effect. Ring statistics were generated using the R.I.N.G.S. code [52], employing Guttman's shortest path criterion [53].

3. Results and discussion

We previously identified a small energy window (10–25 eV) in which Ar-ion bombardment of a nucleating SWCNT cap was found to enlarge the carbon network [25]. In contrast, we here focus on the possible beneficial effects of ion bombardment on the carbon network after cap detachment.

In Fig. 1, we show an example of the beneficial effect of ion bombardment on the network structure, for an impact energy of 20 eV. Indeed, the network structure seems to have improved due the ion irradiation. This is substantiated below.

In Fig. 2, we present the global effect of low-energy ion bombardment on the average number of pentagons and hexagons in the irradiated structure for ions in the energy range of 10–50 eV. The number of pentagons in the structure is actually higher that what is expected for a clean CNT, which is a direct result of the insufficient defect healing during the nucleation and growth stage, which in turn results from the very high growth rate in the simulation. Note that the number of heptagons in the structure is also fairly large, for the same reason, but it nearly remains constant under ion irradiation (see also Fig. 3 below), and is therefore not shown in this figure for clarity.

We can see in the figure that the number of pentagons and especially hexagons increases due to the ion impact at 10 eV, and the number of both rings clearly rises at 25 eV. On the other hand, it remains more or less constant at 40 eV, and decreases at 50 eV. If we identify an increase in the number of (pentagons and) hexagons in the network as a positive effect, we may thus infer from this result that ion irradiation of growing SWCNT is beneficial below 40 eV.

We plot in Fig. 3 the evolution of all the rings detected in the network (i.e., triangles up to nonagons) as a function of the number of ion impacts for an ion impact energy of 20 eV. As also expected from Fig. 2, we find that the number of hexagons and pentagons increases at this ion energy, on average by 29.2% and 20.0%, respectively, for 200 impacts. The beneficial effect of the ion irradiation, however, is not limited to the formation of new graphene-like rings (pentagons and hexagons), but is also evident from the reduction in the number of non-graphene-like rings (triangles, octagons and nonagons). At 20 eV, the change in the number of triangles, octagons and nonagons is −77.5%, −35% and −60%, respectively, after 200 impacts.

The ion bombardment thus has two important effects: (1) the graphitic network is enlarged (formation of graphene-like rings), and (2) at the same time, the defects in the network are reduced (removal of non-graphene-like rings).

In Fig. 4, we show the percentage change in the number of hexagons and in the ratio of hexagons to the total number of

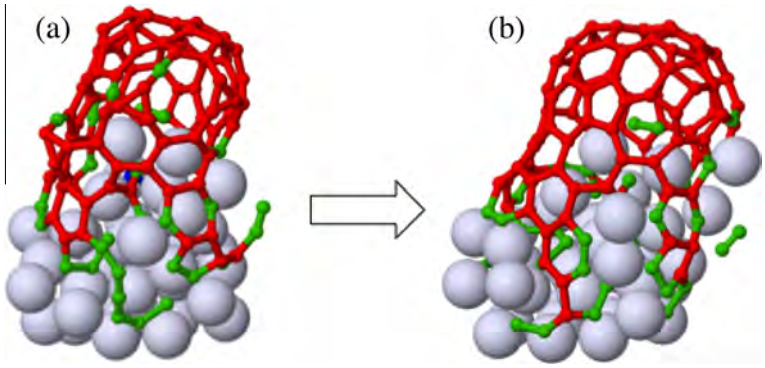

Fig. 1 – Initial structure prior to ion bombardment (a), and carbon network after 200 Ar impacts at 20 eV (b). The big grey spheres represent Ni atoms, and the green and red small spheres represent 2-coordinated and 3-coordinated C atoms, respectively. The graphitic network structure is indeed clearly improved in (b). (A color version of this figure can be viewed online.)

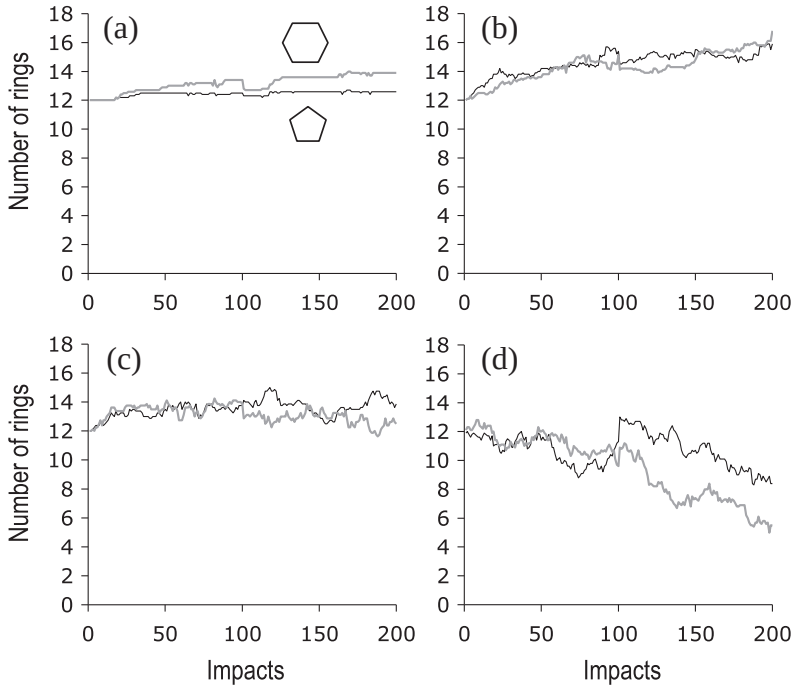

Fig. 2 – Evolution of the number of pentagons and hexagons in the carbon network upon ion impact, as a function of the impact number at (a) 10 eV; (b) 25 eV; (c) 40 eV; and (d) 50 eV, averaged over 10 independent runs. The thick grey lines and thin black lines represent the number of hexagons and pentagons, respectively.

rings, after 200 impacts, for different ion impact energies. The figure demonstrates that an optimum is reached at an impact energy of 25 eV, with an increase in the number of hexagons of 40%. The increase in the ratio of the number of hexagons to the total number of rings is 27.5% at 25 eV. It is also clear from the figure that the number of hexagons as well as the aforementioned ratio only starts to decrease at 50 eV, relative to the initial structure. Note that these results indicate a shift in optimal energy to higher values compared to our earlier simulations for a carbon network in contact with the metal nanoparticle [25].

As a typical example of graphitic network improvement upon ion bombardment, we picture the evolution of a graphitic patch in the network in Fig. 5, as evolving under the action of the ion bombardment at 20 eV. For the sake of clarity, only the graphitic rings are shown, and not the carbon chains or other carbon atoms connected to them. The reader can see how the network gradually expands from a single hexagon to a patch of 6 rings, consisting of 4 hexagons and 2 pentagons, required for the curvature on the nanoparticle surface.

Finally, in Fig. 6, we show the change in the number of carbon atoms in the CNT structure due to the ion bombardment as a function of the ion impact energy. The number of carbon atoms decreases on average by 0.6% at 10 eV, 1.9% at 20 eV, 2.9% at 25 eV, 4% at 30 eV, 10% at 35 eV and even 32% at 50 eV. Thus, sputtering of carbon atoms becomes important from about 35 eV.

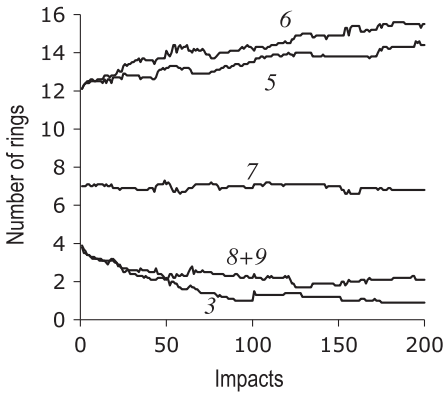

Fig. 3 – Evolution of the number of various rings detected in the structure upon ion impact, as a function of the number of ion impacts, for an ion impact energy of 20 eV, averaged over 10 independent runs. The increase in number of pentagons and hexagons, the constant number of heptagons, and the decrease in the number of octagons, nonagons and triangles is characteristic for all impingement energies in the range 10–25 eV.

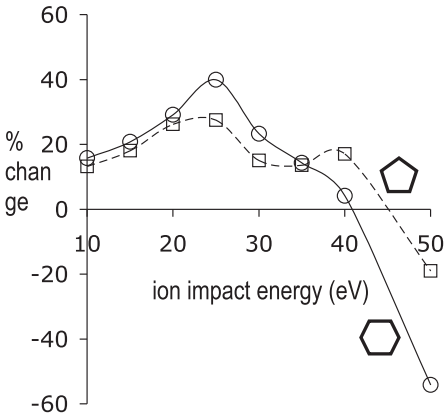

Fig. 4 – Percent change in the number of hexagons (open circles, solid line) and ratio of the number of hexagons to the total number of rings (open squares, dashed line), as resulting from 200 consecutive Ar ion impacts, as a function of the ion impact energy. It can be seen that the beneficial effect of ion bombardment on the C-network structure is at a maximum at 25 eV.

This is indeed as expected based on earlier findings. Indeed, the carbon displacement energy in graphitic structures is in the range 14–32 eV [11,54–56]. Given that the kinetic energy mass transfer factor for Ar/C collisions is 71%, an Ar impact energy of 35–40 eV corresponds to a threshold C-displacement energy of about 25–28 eV. As also mentioned in our previous study [25], the network is, however, far from perfect, and some carbon displacements and limited network damage may already occur at lower impact energies, due to the non-ideal network coordination and structure. In most cases, however, the network is improved at these lower energies, a representative example of which was shown in Fig. 1 for an ion impact energy of 20 eV.

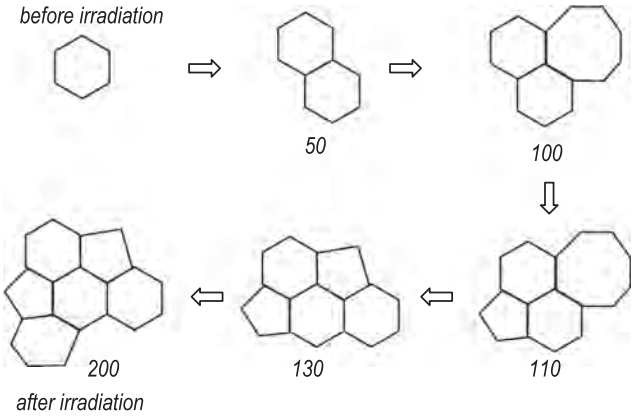

Fig. 5 – Illustration of the graphitic network improvement due to ion bombardment for an ion impact energy of 20 eV. For clarity, only the rings involved in the graphitic network formation are shown. The number of impacts after which each structure was obtained is indicated below each structure.

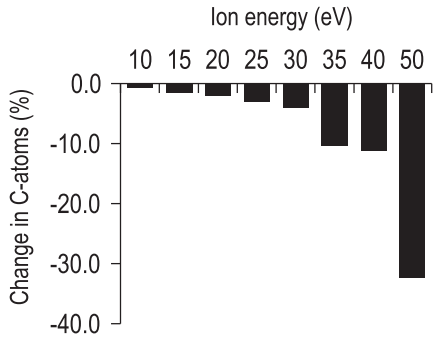

Fig. 6 – Calculated change in the number of carbon atoms in the total structure after 200 Ar impacts as a function of the impact energy.

All of these data point towards a balance between ring formation on one hand, and carbon removal and bond dissociation on the other hand. At an ion impact energy of around 35–40 eV, both effects balance each other, resulting in no network improvement or destruction. At higher energies, above 40 eV, the CNT structure is sputtered and the number of rings decreases. On the other hand, at lower energies, i.e., below 35 eV, the CNT-network is enlarged by the increase in pentagons and hexagons, and the concurrent removal of defects from the network.

4. Conclusions

Employing state-of-the-art reactive molecular dynamics simulations, we demonstrate that low energy ion irradiation of a growing SWCNT structure, not in contact with the metal nanocluster, results in an increase in the number of graphitic rings and a decrease in the number of non-graphitic rings, i.e., in defect healing. We estimate that the ion energy at which there is a balance between defect healing and defect formation is around 35–40 eV. Below this energy, there is a net healing of defects, whereas above this energy, there is a

net formation of defects. We therefore conclude that SWCNT growth in a plasma setup is feasible, provided that the ion peak energy is below 40 eV.

Acknowledgments

This work was carried out using the Turing HPC infrastructure at the CalcUA core facility of the Universiteit Antwerpen (UA), a division of the Flemish Supercomputer Center VSC, funded by the Hercules Foundation, the Flemish Government (department EWI) and the UA.

REFERENCES

[1] Schnorr JM, Swager TM. Emerging applications of carbon nanotubes. Chem Mater 2011;23:646–57.
[2] Baughman RH, Zakhidov AA, de Heer WA. Carbon nanotubes – the route toward applications. Science 2002;297:787–92.
[3] Skakalova V, Dettlaff-Weglikowska U, Roth S. Gamma-irradiated and functionalized single wall nanotubes. Diamond Relat Mater 2004;13:296–8.
[4] Hulman M, Skakalova V, Roth S, Kuzmany H. Raman spectroscopy of single-wall carbon nanotubes and graphite irradiated by gamma rays. J Appl Phys 2005;98:024311.
[5] Zobelli A, Gloter A, Ewels CP, Colliex C. Shaping single walled nanotubes with an electron beam. Phys Rev B 2008;77:045410.
[6] Kis A, Csanyi G, Salvetat J-P, Lee T-N, Couteau E, Kulik AJ, et al. Reinforcement of single-walled carbon nanotube bundles by intertube bridging. Nat Mater 2004;3:153–7.
[7] Tolvanen A, Kotakoski J, Krasheninnikov AV, Nordlund K. Relative abundance of single and double vacancies in irradiated single-walled carbon nanotubes. Appl Phys Lett 2007;91:173109.
[8] Talapatra S, Ganesan PG, Kim T, Vajtai R, Huang M, Shima M, et al. Irradiation-induced magnetism in carbon nanostructures. Phys Rev Lett 2005;95:097201.
[9] Jung YJ, Homma Y, Vajtai R, Kobayashi Y, Ogino T, Ajayan PM. Straightening suspended single walled carbon nanotubes by ion irradiation. Nano Lett 2004;4:1109–13.
[10] Krasheninnikov AV, Nordlund K, Keinonen J, Banhart F. Ion-irradiation-induced welding of carbon nanotubes. Phys Rev B 2002;66:245403.
[11] Krasheninnikov AV, Banhart F, Li JX, Foster AS, Nieminen RM. Stability of carbon nanotubes under electron irradiation: role of tube diameter and chirality. Phys Rev B 2005;72:125428.
[12] Terrones M, Banhart F, Grobert N, Charlier J-C, Terrones H, Ajayan PM. Molecular junctions by joining single-walled carbon nanotubes. Phys. Rev. Lett. 2002;89:075505.
[13] Kim D-H, Jang H-S, Kim C-D, Cho D-S, Kang H-D, Lee H-R. Enhancement of the field emission of carbon nanotubes straightened by application of argon ion irradiation. Chem Phys Lett 2003;378:232–7.
[14] Raghuveer MS, Ganesan PG, D'Arcy-Gall J, Ramanath G, Marshall M, Petrov I. Nanomachining carbon nanotubes with ion beams. Appl Phys Lett 2004;84:4484–6.
[15] Krasheninnikov AV, Banhart F. Engineering of nanostructured carbon materials with electron or ion beams. Nat Mater 2007;6:723–33.
[16] Banhart F, Li JX, Terrones M. Cutting single-walled carbon nanotubes with an electron beam: evidence for atom migration inside nanotubes. Small 2005;1:953–6.
[17] Terrones M, Terrones H, Banhart F, Charlier J-C, Ajayan PM. Coalescence of single-walled carbon nanotubes. Science 2000;288:1226–9.
[18] Wei BQ, D'Arcy-Gall J, Ajayan PM, Ramanath G. Tailoring structure and electrical properties of carbon nanotubes using kilo-electron-volt ions. Appl Phys Lett 2003;83:3581–3.
[19] Yuzwinsky T, Fennimore A, Mickelson W, Esquivias C, Zettl A. Precision cutting of nanotubes with a low-energy electron beam. Appl Phys Lett 2005;86:053109.
[20] Suzuki M, Ishibashi K, Toratani K, Tsuya D, Aoyagi Y. Tunnel barrier formation using argon-ion irradiation and single quantum dots in multiwall carbon nanotubes. Appl Phys Lett 2002;81:2273–5.
[21] Schittenhelm H, Geohegan DB, Jellison GE, Puretzky AA, Lance MJ, Britt PF. Synthesis and characterization of single-wall carbon nanotube-amorphous diamond thin-film composites. Appl Phys Lett A 2002;81:2097–9.
[22] Neyts EC. PECVD growth of carbon nanotubes: from experiment to simulation. J Vacuum Sci Technol B 2012;30:30803.
[23] Ostrikov K, Neyts EC, Meyyappan M. Plasma nanoscience: from nano-solids in plasmas to nano-plasmas in solids. Adv Phys 2013;62:113–224.
[24] Gohier A, Minea TM, Djouadi MA, Jimenez J, Granier A. Growth kinetics of low temperature single-wall and few walled carbon nanotubes grown by plasma enhanced chemical vapor deposition. Physica E 2007;37:34–9.
[25] Neyts EC, Ostrikov K, Han ZJ, Kumar S, Van Duin ACT, Bogaerts A. Defect healing and enhanced nucleation of carbon nanotubes by low-energy ion bombardment. Phys Rev Lett 2013;110:65501.
[26] Ni B, Andrews R, Jacques D, Qian D, Wijesundara MBJ, Choi Y, et al. A combined computational and experimental study of ion-beam modification of carbon nanotube bundles. Appl Phys A 2001;105:12719–25.
[27] Krasheninnikov AV, Nordlund K, Keinonen J. Carbon nanotubes as masks against ion irradiation: an insight from atomistic simulations. Appl Phys Lett 2002;81:1101–3.
[28] Krasheninnikov AV, Nordlund K, Sirvio M, Salonen E, Keinonen J. Formation of ion-irradiation-induced atomic-scale defects on walls of carbon nanotubes. Phys Rev B 2001;63:245405.
[29] Krasheninnikov AV, Nordlund K, Keinonen J. Production of defects in supported carbon nanotubes under ion irradiation. Phys Rev B 2002;65:165423.
[30] Xu Z, Zhang W, Zhu Z, Huai P. Molecular dynamics study of damage production in single-walled carbon nanotubes irradiated by various ion species. Nanotechnology 2009;20:125706.
[31] Xu Z, Zhang W, Zhu Z, Ren C, Li Y, Huai P. Effects of tube diameter and chirality on the stability of single-walled carbon nanotubes under ion irradiation. J Appl Phys 2009;106:043501.
[32] Krasheninnikov AV, Nordlund K, Salonen E, Keinonen J, Wu CH. Sputtering of amorphous hydrogenated carbon by hyperthermal ions as studied by tight-binding molecular dynamics. Comput Mater Sci 2002;25:427–34.
[33] Pomoell J, Krasheninnikov AV, Nordlund K, Keinonen J. Stopping of energetic ions in carbon nanotubes. Nucl Instrum Methods Phys Res B 2003;206:18–21.
[34] Krasheninnikov AV, Miyamoto Y, Tomanek D. Role of electronic excitations in ion collisions with carbon nanostructures. Phys Rev Lett 2007;99:016104.
[35] Pomoell JAV, Krasheninnikov AV, Nordlund K, Keinonen J. Ion ranges and irradiation-induced defects in multiwalled carbon nanotubes. J Appl Phys 2004;96:2864–71.
[36] Kotakoski J, Krasheninnikov AV, Ma Y, Foster AS, Nordlund K, Nieminen RM. B and N ion implantation into carbon nanotubes: insight from atomistic simulations. Phys Rev B 2005;71:205408.

[37] Krasheninnikov AV, Nordlund K. Irradiation effects in carbon nanotubes. Nucl Instrum Methods Phys Res B 2004;216:355–66.
[38] Kotakoski J, Pomoell JAV, Krasheninnikov AV, Nordlund K. Irradiation-assisted substitution of carbon atoms with nitrogen and boron in single-walled carbon nanotubes. Nucl Instrum Methods Phys Res B 2005;228:31–6.
[39] O'Brien NP, McCarthy MA, Curtin WA. Improved inter-tube coupling in CNT bundles through carbon ion irradiation. Carbon 2013;51:173–84.
[40] Salonen E, Krasheninnikov AV, Nordlund K. Ion-irradiation-induced defects in bundles of carbon nanotubes. Nucl Instrum Methods Phys Res B 2002;193:603–8.
[41] Pregler SK, Sinnott SB. Molecular dynamics simulations of electron and ion beam irradiation of multiwalled carbon nanotubes: the effects on failure by inner tube sliding. Phys Rev B 2006;73:224106.
[42] Pregler SK, Jeong B-W, Sinnott SB. Ar beam modification of nanotube based composites using molecular dynamics simulations. Compos. Sci. Technol. 2008;68:2049–55.
[43] Yuan Q, Xu Z, Yakobson BI, Ding F. Efficient defect healing in catalytic carbon nanotube growth. Phys Rev Lett 2012;108:245505.
[44] Karoui S, Amara H, Bichara C, Ducastelle F. Nickel-assisted healing of defective graphene. ACS Nano 2010;4:6114–20.
[45] Neyts EC, van Duin ACT, Bogaerts A. Changing chirality during single-walled carbon nanotube growth: a reactive molecular dynamics/Monte Carlo study. J Am Chem Soc 2011;133:17225–31.
[46] Neyts EC, Shibuta Y, van Duin ACT, Bogaerts A. Catalyzed growth of carbon nanotube with definable chirality by hybrid molecular dynamics-force biased Monte Carlo simulations. ACS Nano 2010;4:6665–72.
[47] Neyts EC, van Duin ACT, Bogaerts A. Insights in the plasma-assisted growth of carbon nanotubes through atomic scale simulations: effect of electric field. J Am Chem Soc 2012;134:1256–60.
[48] van Duin ACT, Dasgupta S, Lorant F, Goddard III WA. ReaxFF: a reactive force field for hydrocarbons. J Phys Chem A 2001;105:9396–409.
[49] Mueller JE, van Duin ACT, Goddard III WA. Development and validation of ReaxFF reactive force field for hydrocarbon chemistry catalyzed by nickel. J Phys Chem C 2010;114:4939–49.
[50] Neyts E, Bogaerts A, Gijbels R, Benedikt J, van de Sanden MCM. Molecular dynamics simulations for the growth of diamond-like carbon films from low kinetic energy species. Diamond Relat Mater 2004;13:1873–81.
[51] Neyts E, Eckert M, Bogaerts A. Molecular dynamics simulations of the growth of thin a-C: H films under additional ion bombardment: influence of the growth species and the Ar^+ ion kinetic energy. Chem Vap Deposition 2007;13:312–8.
[52] Le Roux S, Jund P. Ring statistics analysis of topological networks: new approach and application to amorphous GeS_2 and SiO_2 systems. Comput Mater Sci 2010;49:70–83.
[53] Guttman L. Ring structure of the crystalline and amorphous forms of silicon dioxide. J Non-Cryst Solids 1990;116:145–7.
[54] Lehtinen O, Kotakoski J, Krasheninnikov AV, Tolvanen A, Nordlund K, Keinonen J. Effects of ion bombardment on a two-dimensional target: atomistic simulations of graphene irradiation. Phys Rev B 2010;81:153401.
[55] Montet GL, Myers GE. Threshold energy for displacement of surface atoms in graphite. Carbon 1971;9:179–80.
[56] Banhart F. Irradiation effects in carbon nanostructures. Rep Prog Phys 1999;62:1181–221.